Effects of temperature, humidity, and air saturation state on the transmission risk prediction of COVID-19 in typical scenarios

Ning Mao
Sichuan University - Wangjiang Campus: Sichuan University
Dingkun Zhang
Sichuan University West China Hospital
Yupei Li
Sichuan University - Wangjiang Campus: Sichuan University
Ying Li
Sichuan University - Wangjiang Campus: Sichuan University
Jin Li
Sichuan University - Wangjiang Campus: Sichuan University
Li Zhao
China Academy of Building Research
Qingqin Wang
China Academy of Building Research
Zhu Cheng
Sichuan University - Wangjiang Campus: Sichuan University
Yin Zhang
Sichuan University - Wangjiang Campus: Sichuan University
Enshen Long (longes2@163.com)
Sichuan University https://orcid.org/0000-0003-0774-4275

Research Article

Keywords: temperature, relative humidity, air saturation state, COVID-19, respiratory tract deposition, transmission risk model

Posted Date: May 11th, 2022

DOI: https://doi.org/10.21203/rs.3.rs-1525744/v1

Title Page

Effects of temperature, humidity, and air saturation state on the transmission risk prediction of COVID-19 in typical scenarios

Ning Mao[a], Dingkun Zhang[b], Yupei Li[a], Ying Li[c], Jin Li[c], Li Zhao[d], Qingqin Wang[d], Zhu Cheng[c], Yin Zhang[c], Enshen Long[a,c,*]

[a] MOE Key Laboratory of Deep Earth Science and Engineering, Institute of Disaster Management and Reconstruction, Sichuan University, Chengdu, China

[b] Laboratory of Clinical Proteomics and Metabolomics, Institutes for Systems Genetics, West China Hospital, Sichuan University, Chengdu, China

[c] College of Architecture and Environment, Sichuan University, Chengdu, China

[d] China Academy of Building Research, Beijing, China

Corresponding author: Enshen Long

Affiliation: MOE Key Laboratory of Deep Earth Science and Engineering, Institute of Disaster Management and Reconstruction, College of Architecture and Environment, Sichuan University, Chengdu, China.

Mailing address: Room 112, Administration Building, Sichuan University, No. 24, First loop south first section, Chengdu 610065, Sichuan Province, China

Tel: +86 28 85401015; Fax: +86 28 85401015 E-mail address: longes2@163.com

Acknowledgments

This work was supported by the National Natural Science Foundation of China (52078314).

Abstract: Environmental parameters have a significant impact on the spread of respiratory viral diseases. Temperature and relative humidity are correlated with viral inactivation in the air, whereas supersaturated air can promote viral deposition in the respiratory tract. This study introduces a new concept, the dynamic virus deposition ratio (α), that reflects the dynamic changes in particle size and viral deposition under varying ambient environments. Moreover, a non-steady-state modified Wells-Riley model is established to predict the infection risk of shared air space under varying environmental parameters, including temperature, relative humidity, and air saturation state. The quanta emission rate of an asymptomatic infector during different respiratory activities (breath, voice, and cough) are explored, and the differences in the infection risk under saturated and unsaturated air conditions are also compared. Finally, six typical exposure scenarios from daily life are also explored, highlighting scenarios of higher risk. The results show that the highest infection risk (R_{max}=5.2%) and the longest risk duration ($T_{terminal}$=6.8h) are both reached in cold and damp conditions. This study quantitatively reflects how environmental parameters are linked to viral inactivation and particle deposition, affecting transmission risk.

Keywords: temperature; relative humidity; air saturation state; COVID-19; respiratory tract deposition; transmission risk model

Graphical Abstract:

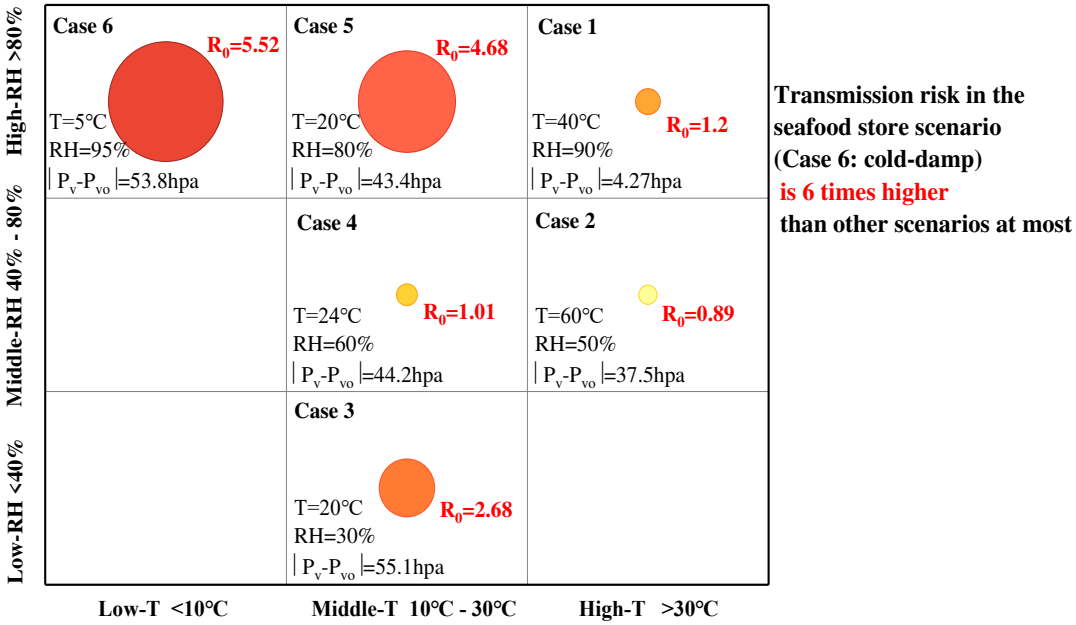

R_0: Basic Reproduction Number T: Temperature RH: Relative Humidity P_v: Saturated vapor pressure

1. Introduction

The novel coronavirus disease 2019 (COVID-19) has stimulated unprecedented public health concerns (Azman &Luquero 2020, Liu et al. 2020b, Morawska et al. 2020). Two years have passed since its early outbreak, COVID-19 prevention has destined to be a prolonged battle. It is impracticable for all human active areas to take long-term disinfection and isolation of activities. Therefore, our attention needs to be directed to high-risk areas. Without considering other artificial factors, an urgent need is to identify the exposure scenarios that may promote COVID-19 transmission.

It has been reported that seasonal cyclicity is a ubiquitous feature of acute infectious diseases, which is also commonly observed in respiratory viral diseases, such as SARS and MERS (Killerby et al. 2018, Lipsitch et al. 2020, Wang et al. 2020). Therefore, it is reasonable to speculate that environmental and meteorological factors affect the COVID-19. To control the pandemic, many studies have examined meteorological/weather conditions that might influence the spread of coronaviruses by exploring the association between these factors and the COVID-19 cases over different worldwide locations, as Table 1 shows (Lin et al. 2020, Liu et al. 2020a, Ma et al. 2020, McClymont &Hu 2021, Pani et al. 2020, Prata et al. 2020, Runkle et al. 2020, Sobral et al. 2020, Wu et al. 2020, Xu et al. 2020). Conclusions regarding the effects of meteorological parameters on COVID-19 transmission are significant, such as air temperature (T), relative humidity (RH) and saturated vapor pressure (P_v) (Franch-Pardo et al. 2020, Ishmatov 2020, Xi et al. 2015). In particular, the argument was further supported by these reports that

employees who worked in cold chain transportation were more vulnerable to diagnosed with COVID-19 (https://baijiahao.baidu.com/s?id=1728401608245389772&wfr=spider&for=pc), and the covering of imported frozen seafood such as salmon (http://finance.sina.com.cn/china/gncj/2020-06-13/doc-iirczymk6749091.shtml) and shrimp (https://www.best73.com/news/27562.html) tested positive for SARS-CoV-2 too.

Table 1 Association of COVID-19 pandemic with meteorological parameters (Lin et al. 2020, Liu et al. 2020a, Ma et al. 2020, McClymont &Hu 2021, Pani et al. 2020, Prata et al. 2020, Runkle et al. 2020, Sobral et al. 2020, Wu et al. 2020, Xu et al. 2020)

Area	Influence factor	COVID-19	Result	Reference
Singapore	Temperature, relative humidity, absolute humidity, and water vapor	Confirmed cases	Temperature, dew point, and absolute humidity showed positive significant associations with transmission	(Pani et al. 2020)
Brazil	Temperature,	Confirmed cases	When the average temperature < 25.8 C, each 1°C rise was associated with a 4.9% decrease in COVID-19 confirmed cases	(Prata et al. 2020)
China	Temperature, diurnal temperature range, absolute humidity, and migration scale index (MSI)	Confirmed cases	The weather with low temperature, mild diurnal temperature range and low humidity likely favors the transmission of COVID-19	(Liu et al. 2020a)
China	Temperature, population density	Scaled Transmission Rate (STR)	COVID-19 mitigation in densely populated and cold regions will be a great challenge	(Lin et al. 2020)
China	Temperature, relative humidity, and air quality index (AQI)	Confirmed cases	Impact of AQI on the spread of COVID-19 may be enhanced under low relative humidity.	(Xu et al. 2020)
the US	Temperature, solar, and specific humidity	Confirmed cases	Short-term exposure to humidity was positively associated with COVID-19 transmission	(Runkle et al. 2020)
Whole world	Temperature, diurnal temperature range, and precipitation	Confirmed cases and deaths	There was a negative correlation between the average temperature and the number of cases of infections.	(Sobral et al. 2020)
166 countries	Temperature, and relative humidity	Confirmed cases and deaths	A 1 °C increase in temperature was associated with a 3.08% reduction in cases	(Wu et al. 2020)
China	Temperature, relative humidity, and air pollutant	Daily death counts	One unit increase in diurnal temperature range was associated with a 2.92% increase in COVID-19 deaths	(Ma et al. 2020)

However, the association between meteorological parameters and COVID-19 cases also would be

affected by local artificial factors, including social, political, and economic (Lai et al. 2020). The results in quantifying environment effects on transmission risk is limited and equivocal.

Therefore, to reject the effect of other social factors, quantifiable mathematical models of transmission risk are needed (Bin et al. 2018, Borro et al. 2020, Qian et al. 2012, Sharma &Balasubramanian 2020). Wells-Riley model (W-R model) is one of the most popular models for quantitatively assessing the infection risk of airborne diseases (Keene 1955, Riley et al. 1978, Vuorinen et al. 2020, Wagner et al. 2009, Zhang et al. 2020). Understandably, the W-R model has been further improved and extended by many latest studies, to include more realistic factors and considerations since the COVID-19 outbreak. For instance, Nordsiek et al. developed an optimization W-R model for computational risk assessment suitable for mono/poly-pathogen aerosols (Nordsiek et al. 2021). Andrews et al. used a modified W-R model to estimate the impact of ventilation on infection probability for inmates sharing a cell with an infector (Urrego et al. 2015). Zhou and Koutsopoulos proposed a modified W-R model for risk analysis in public transportation systems, which integrated with a simulation model of subway operations (Zhou &Koutsopoulos 2021). Zhai et al. and Zhang et al. developed modified W-R model for integrating the spatial distribution of pathogen concentrations (Guo et al. 2021, Zhai &Li 2021). Fierce et al. tried to developed the Quadrature-based model of droplets risk by introducing a dose-response framework, which could reflect the evolution of particles after they are expelled, their deposition in the airways, and the subsequent risk of initial infection (Fierce et al. 2021).

Although the various studies above used different methods for risk analysis of airborne diseases, they collectively treated the shared air space as a close-to-greenhouse environment. The T, RH, and P_v are assumed to be constant. However, the epidemic outbreak in different regions and keep transmitting under varying environmental parameters. It can be seen from Table 1 those environmental parameters were believed to significantly promote or inhibit the spread of COVID-19. Therefore, a non-steady-state modified Wells-Riley model the dynamic change of environmental parameters is required.

This study aims to answer the following questions: How are T, RH, and P_v linked to infection risk? Which exposure scenarios promote or inhibit COVID-19 transmission? The answers to these questions will help local healthcare policymakers grade human activity regions according to the COVID-19 transmission risk.

2. Methodology

As stated above, a non-steady-state modified Wells-Riley model under varying environments is required. To address this need, the key environmental parameters which influence the infection risk of airborne diseases are determined during the full cycle of droplets transmission in the shared air space (T, RH, and P_v). Firstly, T and RH are closely related to viral inactivation rate in the air (λ). The

supersaturated air can promote particle diameter growth in the respiratory tract of susceptible population and, consequently, influence the particle deposition and virion exposure (Xi et al. 2015). Therefore, we introduce a new concept, the dynamic virus deposition ratio (α) that reflects the dynamic changes of virus deposition in supersaturation air state (P_v). We next discuss the derivation process of the non-steady-state modified W-R model under the dynamic change of environmental parameters, as shown in Fig. 1.

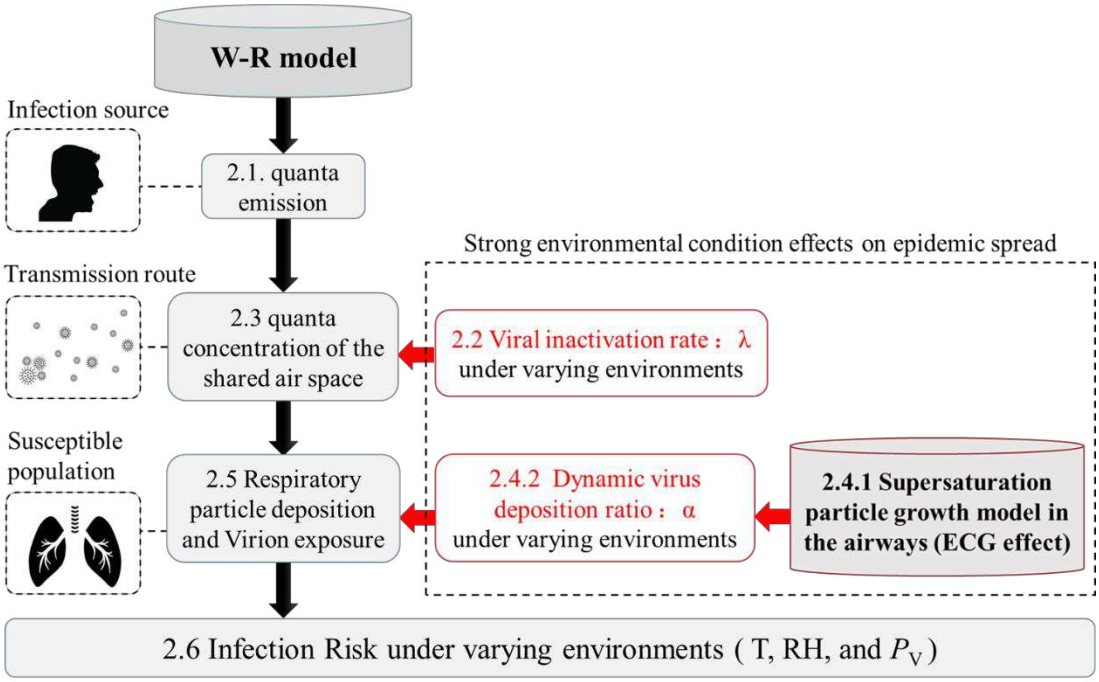

Fig. 1 Derivation of the non-steady-state modified W-R model under the dynamic change of environmental parameters. Enhanced condensational growth (ECG effect) is a concept of pulmonary drug delivery in which the drug aerosol is inhaled combination with cold-supersaturated air. The subsequent small particle condensation growth will promote lung drug deposition (Xi et al. 2015). Similarly, ECG effect would increase the virus deposition risk of airborne diseases.

2.1 quanta emission

A thorough understanding of infectious droplets is a primary factor in the study of COVID-19 airborne transmission risks, such as the diameter distribution, SARS-CoV-2 viral load, and spatiotemporal variation in virion concentrations. It has been reported that the diameter of exhaled droplets mainly ranges between 0.3 and 100 μm, and the number of particles decreases with the increase in droplet diameter (see Appendix A: Table A.1) (Duguid 1946, Lindsley et al. 2012, Morawska et al. 2009). The viral load in body fluids generally peaks approximately 4 to 6 days after onset, up to 10^8 RNA

copies/mL, and then decreases over time (see Appendix A: Table A.2) (Cao et al. 2020, Chen et al. 2020, L. Zou 2020, Y. Pan 2020).

In the original W-R model, the quanta emission rate remains uncertain and highly variable (Gba et al. 2020, Harrichandra et al. 2020). To estimate the spatiotemporal variation in virion concentrations, Buonannoa developed a modified W-R model based on a dose-response method to calculate the virion emission rate through a mass balance, which allows consideration of per-particle variation in viral load and the airborne transmission risk between scenarios (Buonanno et al. 2020). In particular, the viral load emitted was expressed in terms of the quanta emission rate (ER).

$$ER_j = C_V \cdot C_i \cdot p \cdot \sum_{\substack{1 \le i \le n \\ 1 \le j \le m}} (N_{ij} \cdot V_i(d_0)) \quad (1)$$

where ER_j is the quanta emission rate from different respiratory activities (quanta h^{-1}), A quantum is defined as the dose of airborne droplet nuclei required to cause infection in 63% of susceptible persons, j indicates the different expiratory activities considered (breath = 1, voice = 2, cough = 3), C_v is the viral concentration in the throat of the asymptomatic infector (RNA copies/mL), C_i is a conversion factor defined as the ratio between one infectious quantum and the infectious dose expressed in viral RNA copies (Li et al. 2010, Watanabe et al. 2010, Yu et al. 2004) (0.01–0.1), p is the breathing rate per person (Marmett et al. 2020) (m^3/s), N_{ij} is the number of droplets with i diameter from j respiratory activities, and $V_i(d_0)$ is the volume of a single droplet (mL) as a function of the droplet diameter (d_0), the droplets are assumed to be standard spheres.

2.2 Viral inactivation rate in the air

The significant changes in virus survival balance after being exhaled from the infector also lead to differences in the disease infection risk in different environments (Pica &Bouvier 2012, van Doremalen et al. 2020, Wei &Li 2016). Therefore, several scholars have conducted studies on aerosolized viral inactivation under varying T and RH, and aerosolized the viruses into a rotating drum, where the aerosols were held at the desired T and RH. Following this, the samples of air from the drum were collected using an impinger (Doremalen et al. 2013, Pyankov et al. 2018, Sattar et al. 1984). This study summarizes viral inactivation characteristic of respiratory disease under varying T and RH, as shown in Fig. 2.

When T was in a specific value (22 °C–25 °C), the viruses were found to survive better at low RH levels (< 33 %) and high RH levels (> 85 %). The middle RH level (50%–75%) was found to be the least favorable for the survival of the viruses. And, within the range of certain RH, there was significant negative correlation between the viral inactivation rate and T (Colas de la Noue et al. 2014, Harper G. 1961, Lin &Marr 2020, Noti et al. 2013). Therefore, viral inactivation rate in air (λ), is significantly affected by the ambient T and RH, which further inhibits or promotes the spread of an epidemic in local

areas (Mao et al. 2020, Walsh et al. 2020).

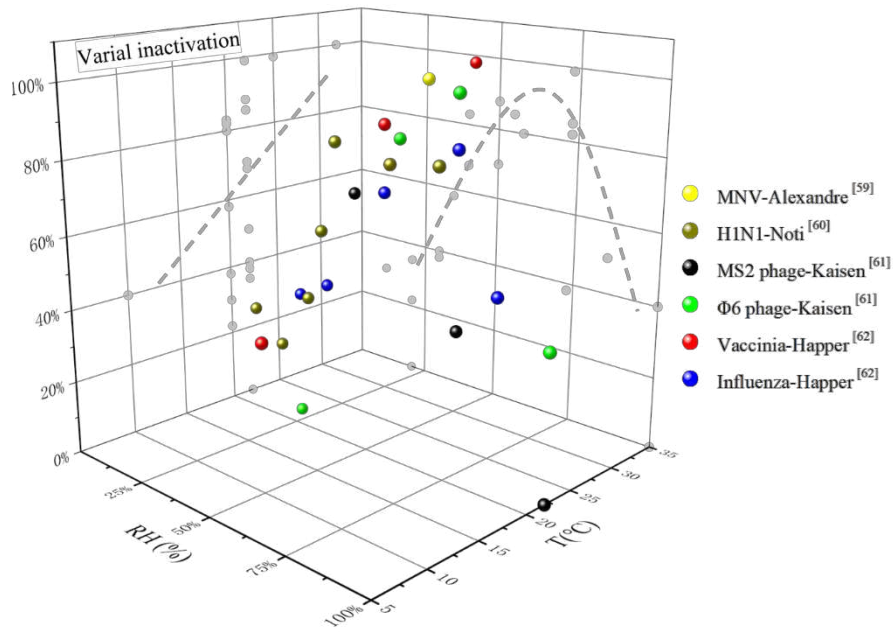

Fig. 2 Aerosolized viral inactivation of respiratory disease in the air (λ, exposure for 1 h). Color spherical point shows the viral inactivation rate for each environment condition, whereas the gray dashed lines show the inactivation trend under the only T condition and only RH condition, respectively. The high T (30 °C–35 °C) and the middle RH level (45%–60%) were found to be the least favorable for the survival of the respiratory disease viruses. For more detailed data, see Appendix A: Table A.3.

2.3 quanta concentration of the shared air space

After being exhaled from the infector, the quanta concentration at time t (Gammaitoni &Nucci 1997), n(t), as follows:

$$n(t)_j = \frac{ER_j \cdot I}{(AER+K+\lambda)\cdot V}\left(1 - e^{-(AER+K+\lambda)\cdot t}\right) \quad (2)$$

where $n(t)_j$ is the quanta concentration from different respiratory activities at time t, I is the number of asymptomatic infectors, AER is the air exchange rate via ventilation (natural ventilation(Alfano et al. 2012, Stabile et al. 2017), 0.2 h^{-1}), K is the particle deposition on surfaces (released from 1.5m at a speed of 1×10^{-4} m/s (Chatoutsidou &Lazaridis 2019), 0.24 h^{-1}), λ is the viral inactivation rate of respiratory disease (the values were selected according to Appendix A: Table A.3), V is the volume of the shared air space(m^{-3}), and t is the exposure time (s).

2.4 Supersaturation particle diameter growth model

2.4.1 Particle deposition in airways (ECG effect)

To analyze pulmonary drug delivery, plenty of studies on particle deposition in the airways have been conducted by medical scholars (Austin et al. 2010, Gralton et al. 2011, Knight 2010, Morrow 2010, Nicas et al. 2005, Yeh &Raabe 1976). During inhalation, when the respiratory tract air (T=37 °C, RH=99% (Winkler-Heil et al. 2017)) is mixed with the inhaled ambient air (relatively low RH and T), the small particle (<10 μm) can grow owing to condensation. The diameter growth factors of inhaled supersaturation droplets in the airways are summarized (Kim et al. 2013, Kreyling 1984, Longest et al. 2011, Sarangapani &Wexler 1996, Xi et al. 2013, Xi et al. 2015) (see Appendix A: Table A.4, and Figure A.1). Therefore, the concept of enhanced condensational growth (ECG effect) was proposed in which a drug aerosol is inhaled in combination with cold-saturated air; this would cause the small particle diameter to increase thereby promoting lung drug deposition (Deng et al. 2020, Longest &Hindle 2010, 2011, Longest et al. 2011, Tian et al. 2011). Understandably, ECG effect would also increase the virus deposition risk of airborne diseases.

It is known that viruses can only cause infection when inhaled by susceptible populations and when successfully deposited in the respiratory tract (Akhbarizadeh et al. 2021, Pu et al. 2020). Furthermore, the deposition fraction of infectious droplets is dependent on the aerosol droplet diameter distribution (Asgari et al. 2019, Fröhlich-Nowoisky et al. 2016). Fig. 3 summarizes the distribution of exhaled droplets from different respiratory activities and the corresponding deposition fractions in the respiratory tract (Protection 1994). It is noteworthy that supersaturated air can lead to significant growth in inhaled small particle diameter in the airways due to the ECG effect. For example, the total deposition of 0.3 μm particles in the airways may rise from 13% (when supersaturation is not considered) to 90% (under supersaturated conditions). It is evident that the infection risk is set to surge.

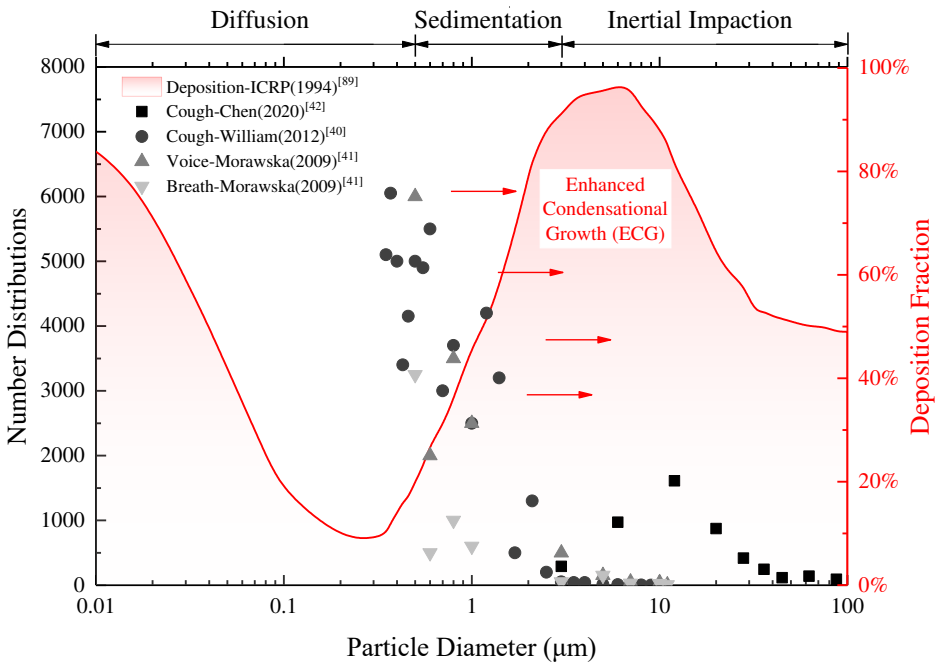

197

198 **Fig. 3 Number distribution of exhaled droplets from different respiratory activities and the**
199 **corresponding deposition fraction in the respiratory tract. Large particles are mainly deposited**
200 **through inertial impaction, whereas small particles are mainly deposited through molecular**
201 **diffusion (Fröhlich-Nowoisky et al. 2016). The ECG effect can lead to significant diameter growth**
202 **of small particle (<10 μm) in the airways. It is evident that the deposited risk was set to surge.**

203 2.4.1 Dynamic virus deposition ratio

204 Considering the dynamic changes in particle size and viral deposition in different ambient
205 environments, our study proposes a new term, the dynamic virus deposition ratio α (Equation 3), which
206 is defined as the ratio between the viral load deposited in the respiratory tract under varying environments
207 ($Q_{deposition}$) and the total viral load inhaled by a Susceptible population (Q_{total}).

208 $$\alpha = \frac{Q_{deposition}}{Q_{total}} \quad (3)$$

209 where $Q_{deposition}$ is the viral load deposited in the respiratory tract under varying ambient
210 environments (RNA copies), and Q_{total} is the total viral load inhaled by a Susceptible population (RNA
211 copies).

212 $$Q_{deposition} = \sum_{i=1}^{n}(C'_{V.i} \cdot p \cdot N'_i \cdot V'_i(d) \cdot \omega'_i) \quad (4)$$

213 $$Q_{total} = \sum_{i=1}^{n}(C_V \cdot p \cdot N_i \cdot V_i(d_0)) \quad (5)$$

where $C'_{V.i}$ is the viral concentration of droplets with i diameter after considering the ECG effect on particle size (RNA copies/mL), N'_i is the number of droplets with i diameter after considering the ECG effect on particle size (part. m−3), $V'_i(\mathrm{d})$ is the volume of a single droplet (mL) as a function of the droplet diameter after considering the ECG effect on particle size (d), and ω'_i is the deposition fraction of droplets with i diameter after considering the ECG effect on particle size (the values were selected according to the ICRP data (Protection 1994)).

The supersaturation diameter growth factors for inhaled air with different saturated vapor pressures (d/d_0) can be calculated from the following equation (Xi et al. 2015):

$$\frac{d}{d_0} = 1 + \frac{0.865 \cdot |P_v - P_{v.o}|^{0.293}}{d_i^{1.13}} \quad (6)$$

where P_v is the saturated vapor pressure of the ambient air (hPa), and $p_{v.o}$ is the saturated vapor pressure of air in the respiratory tract (T=37 °C, RH=99%, P_v=62.1hPa).

However, droplet condensation in the airways (ECG effect) changes their particle size (d'_i), which modifies the concentration of viral charges in the droplets ($C'_{V.i}$, copies/mL) due to a higher liquid fraction. Meanwhile, it should not change the absolute number of viral copies in the droplet (For example, a 1 μm droplet has the same number of viral charges after condensation, whereas their concentration is reduced owing to a higher liquid volume). Therefore, the absolute number of viral copies in a droplet with i diameter after considering the ECG effect can only be a dynamic cumulative value (Equation 7), not directly calculated by the original parameters, such as particle size and concentration (Equation 4).

$$Q'_{deposition} = \sum_{i=1}^{n} (C'_{cum.i} \cdot \omega'_i) \quad (7)$$

$$\alpha = \frac{\sum_{i=1}^{n} (C'_{cum.i} \cdot \omega'_i)}{\sum_{i=1}^{n} (C_V \cdot p \cdot N_i \cdot V_i(d_0))} \quad (8)$$

where $C'_{cum.i}$ is the total viral load of droplets with diameter i after considering the ECG effect on the particle size (RNA copies).

2.5 Respiratory particle deposition and Virion exposure

To illustrate the impact of ECG effect on respiratory particle deposition and Virion exposure, this paper presents the calculation process of dynamic virus deposition ratio, α, in typical cold-saturated condition (Example Case: T=5 °C, RH=95%), As shown in Fig. 4.

According to the Equation 6, the droplets diameter would change during inhalation. The smaller the particle size, the bigger growth factor, and only small particle (<10 μm) shows significantly grow (see Fig. 4 a)). It is assumed that these droplets are deposited after condensation, and the final droplets

distribution ranged from 3 μm to 100 μm. This change is unfortunate to reach the high-risk deposition peak in the airways (see Fig. 4 b)). As a result, the number of deposited particles increased by 3 times (see Fig. 4 c)), the dynamic virus deposition ratio, α, of this condition could go as high as 51.94% (see Fig. 4 d)). Thus, it is evident that the virion exposure and infection risk increases dramatically.

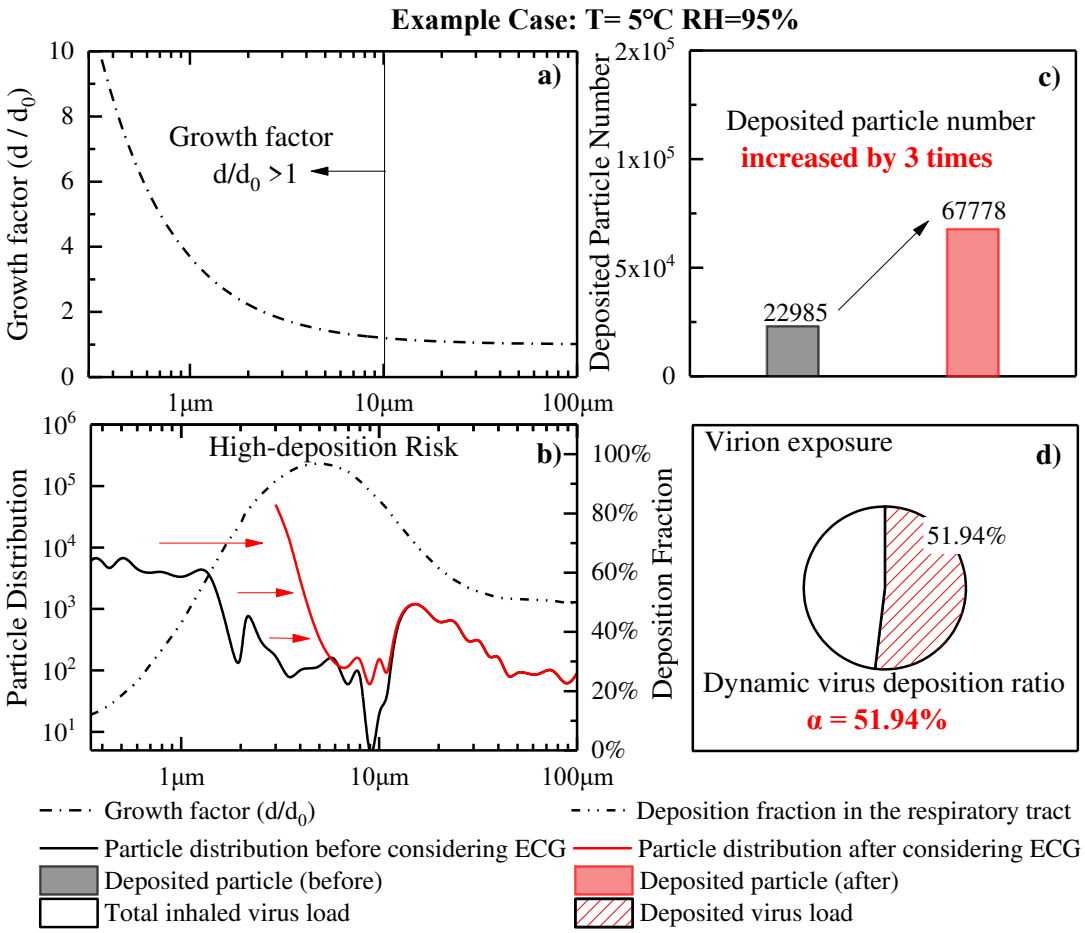

Fig. 4 Calculation process of dynamic virus deposition ratio, α, in typical cold-saturated condition (Example Case: T=5 °C, RH=95%). a). Only small particle (<10 μm) shows significantly grow; b). The grown small particles are unfortunate to reach the high-deposition peak in the airways; c). The deposited particles number increased by 3 times; d). the dynamic virus deposition ratio, α, of this condition could go as high as 51.94%. It is evident that the virion exposure and infection risk increases dramatically.

2.6 Infection Risk under varying environments

Thereafter, the dynamic virus deposition ratio, α, is used to correct the breathing rate of Susceptible population, p, and the modified dimensionless inhalation rate, p', is expected to reflect the dynamic risk due to ECG effect more accurately.

$$p' = p \cdot \alpha \tag{9}$$

Infection risk ($R_{j.t}$, %) as a function of exposure time (t) of susceptible people.

$$R_{j.t} = 1 - \mathrm{e}^{-p\prime \cdot \int_0^t n(t)_j \mathrm{dt}} \tag{10}$$

In the end, the basic reproductive number (R_0) could be calculated if we multiplying the peak of infection risk by the number of all exposed persons during the exposure time (Rothman et al. 2011).

3.Results

3.1 quanta emission rate from different respiratory activities

Fig. 5 shows the ER_j (quanta.h^{-1}) trends as a function of time and viral load in the throat (C_v, Log_{10} RNA copies. mL^{-1}) and the quanta-RNA copies correction factor (C_i, 0.01-0.1) from three respiratory activities (Breath, Voice, Cough) and light exercise activity level (p, 1.38m3/h). For the sole purpose of simplifying the discussion, zones representative of low (< 1 quantum h^{-1}) and high (> 1 quantum h^{-1}) quanta emission are separated by the red dotted line indicated (ER_j, 1 quantum h^{-1}).

The trends of the quanta emission rate are similar to that of the viral load of SARS-CoV-2 in a patient's body fluids, peaking approximately 4 to 6 days after onset and then decreasing over time. In the case involving typical clinical symptoms of the COVID-19 patient (cough condition), the quanta emission rate covers the range of 10^{-4} to 10^5 quanta.h^{-1}, up to 5.55×10^4 quanta.h^{-1}. A high emission in the case of coughing was achieved at 11 days out of 15. Speech is one of the most important communication methods between people (Voice condition). The quanta emission rate covering the range of 10^{-5} to 10^4 quanta.h^{-1}, is approximately 1/10 of the coughing condition. A high emission in the case of speaking can be achieved only at five days out of 15. It is noteworthy that breathing is a continuous behavior of an asymptomatic person during his/her daily activities (breath condition). Although the quanta emission rate fails to achieve a high emission zone in the breath condition, more viruses might accumulate over time due to having a higher frequency than cough and voice conditions.

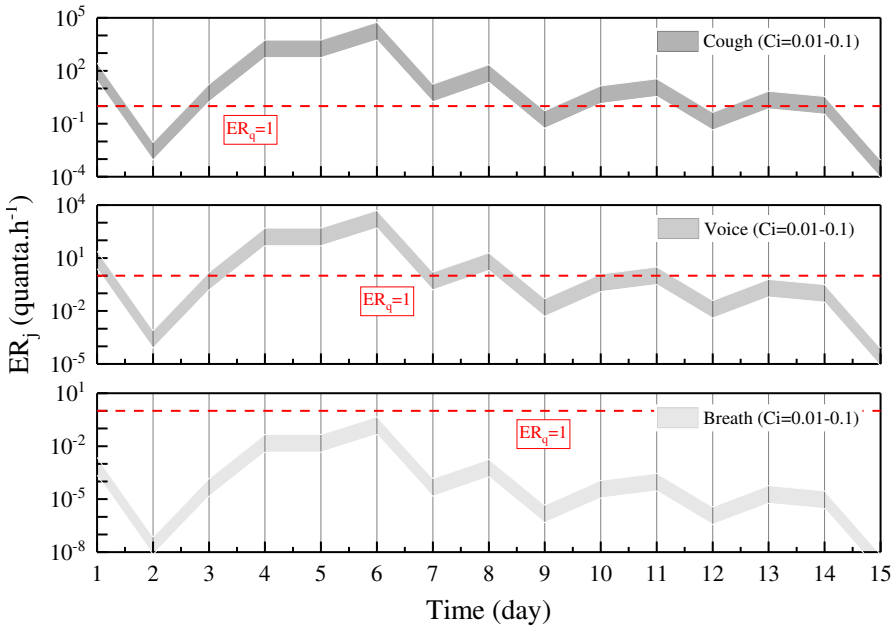

Fig. 5 ER_j (quantum h^{-1}) trends as a function of the time and the viral concentration in throat (C_v, Log_{10} RNA copies.mL^{-1}) and quanta-RNA copies correction factor (C_i, 0.01-0.1) for the three respiratory activities (Breath, Voice, Cough). Only the first 15 days of data are calculated after onset. Zones representative of low (< 1 quantum h^{-1}) and high (> 1 quantum h^{-1}) quanta emission are separated by the red dotted line indicated.

3.2 Infection risk for different environments

This section aims to show how the environmental parameters (T, RH, and P_v) are linked to the disease transmission risk in two different microenvironments, low-temperature saturated condition (Low-T: T=10°C, Saturated: RH=100%, R_{LTS}), and middle-temperature unsaturated condition (Middle-T: T=25°C, Unsaturated: RH=60%, R_{MTUS}).The following input data are defined: C_v is 10^8 RNA copies/mL, AER is 0.2 h^{-1} (natural ventilation (Buonanno et al. 2020)), K is 0.24 h^{-1} (Chatoutsidou &Lazaridis 2019), λ is 0.4 h^{-1} and 0.8 h^{-1} respectively for R_{LTS} and R_{MTUS} (according to Appendix A: Table A.3), Ci is 0.02 (Watanabe et al. 2010), V is 8m*6m*3.5m=168 m^3, and p is 1.38 $m3.h^{-1}$ (light exercise activity level (Adams 1993)). It is assumed that only an asymptomatic infector remained inside the environment for 10 min, the infection risk is simulated for up to 6 h, as shown in Fig. 6.

The trends highlight that the brief stopover of the asymptomatic infector in the microenvironments leads to a peak risk of infection at 10 min. The more intense the respiratory activity, the higher the quanta emission rate. Therefore, the highest disease infection risk was 50% for cough, 6.2% for voice, and 1.2%

for breath. In particular, it is known from the literature mentioned above that the viruses are found to survive better in low-temperature air, and the subsequent particle growth of inhaled supersaturated air promotes lung deposition. Therefore, it is understandable that a higher peak infection risk is reached at R_{LTS} (T=10 ° C, RH=100%) rather than R_{MTUS} (T=25 °C, RH=60%). Cough, ΔR=15±3.3%, p<0.01; Voice, ΔR=2±0.5%, p<0.01; Breath, ΔR=0.0022±0.0006%, p<0.01.

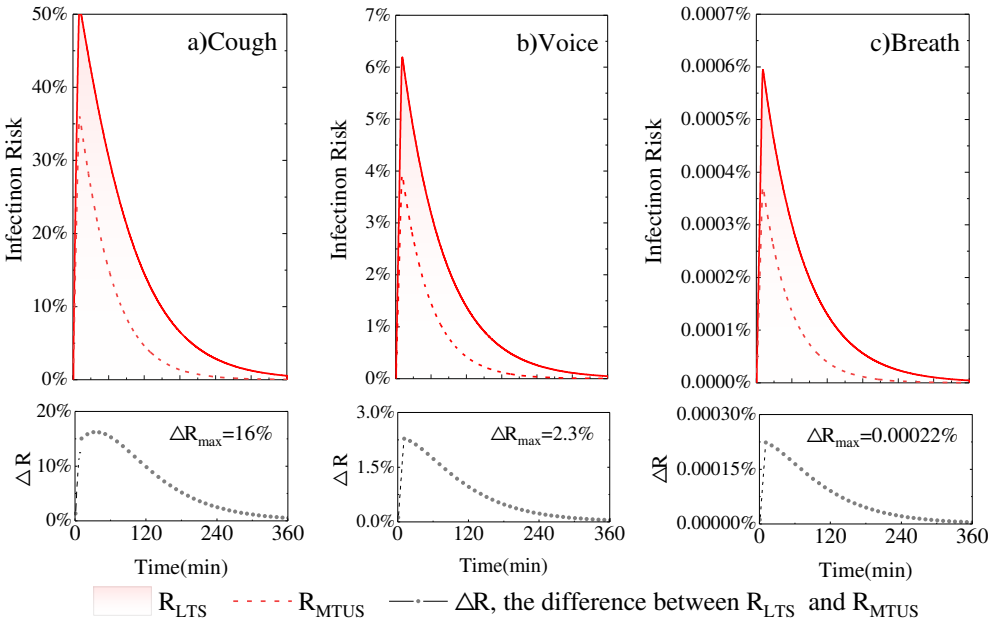

Fig. 6 Infection risk trends as a function of time (an asymptomatic infector remained inside the space for 10 min). The difference (△R) between R_{LTS} (T=10℃, RH=100%) and R_{MTUS} (T=25℃, RH=60%) for three respiratory activities (Cough, Voice, Breath) are compared, respectively.

3.3 Typical scenarios studies

The research results in Section 3.2 support the argument that infection risk varies with the environment. Therefore, six typical exposure scenarios from daily life were chosen to analyze the effects of environmental parameters on disease transmission risk. The control parameters for the different exposure scenarios are summarized in Table 2.

First, the exposure scenarios of the shower room (Case 1, high-T and high-RH conditions (China 1998)), and the sauna (Case 2, high-T and middle-RH conditions (China 1998),) were selected to analyze the infection risk under high temperature. Second, the most common exposure scenario during daily life is selected as a comparison condition (Case 4, middle-T and middle-RH conditions (China 2017)). As the flu season approaches, the indoor exposure scenarios during raining condition in autumn(Case 5, middle-T and high-RH conditions (Nan et al. 2009)),and during heating conditions in winter (Case 3, middle-T and low-RH conditions (Yan 2015)) were selected to analyze the infection risk under middle

temperature. Finally, based on the conclusions in Section 3.2, the infection risk in the scenario (cold and damp) must be taken seriously. Therefore, the extreme typical exposure scenario of the seafood cold store (Case 6, low-T and high-RH conditions (China 2010)) is analyzed.

Table 2 Control parameters for different exposure scenarios

Environment parameters	Case 1	Case 2	Case 3	Case 4	Case 5	Case 6
Temperature [a] (T, ℃)	40	60	20	24	20	5
Relative Humidity [b] (RH, %)	90	50	30	60	80	95
Viral inactivation (λ, h^{-1})	0.8	0.99	0.4	0.9	0.2	0.15
Saturated vapor pressure (P_v, hPa)	66.37	99.64	7.01	17.9	18.7	8.3
Vapor Pressure difference [c] ($\|P_v$-$P_{vo}\|$, hPa)	4.27	37.5	55.1	44.2	43.4	53.8

[a]: High-temperature: T>30℃; Middle-temperature: 10℃<T<30℃; Low-temperature: T<30℃.

[b]: Higher-humidity: RH>80%; middle humidity: 40%<RH<80%; lower humidity: RH<30%.

[c]: Absolute value of the saturated vapor pressure difference between ambient air and respiratory tract air.

Respiratory boundary conditions: T=37 °C, RH=99%, and P_{vo}=62.1 hPa .

For all the typical exposure scenarios considered in the simulations, the asymptomatic infector remains inside the environment for 5 min, as shown in Fig. 7. The aim is to compare the infection risk during speaking (Voice, j=2) in the shared air space. For this reason, the following assumption for all scenarios are defined: 4 persons are always present; 1 new visitor every 5 min enters; every visitor remains inside for 5 min; thus, 5 persons are simultaneously present. The other input data is consistent with section 3.2.

Although the quanta emission rate is consistent in each scenario, viral inactivation in air (λ) and the deposition fraction in the respiratory tract (ω) are significantly influenced by the environment. Thus, remarkable differences in disease transmission between the scenarios are noted. The brief stopover of the asymptomatic infector in the microenvironments leads to a peak risk of infection at 5 min (R_{max}, the peak of infection risk). After the asymptomatic infector leaves, the quanta concentration slowly drops to a safe level (T_{terminal} , the high infection risk duration of the microenvironment). During this period, the number of all the persons who visited the microenvironment is counted (N_{max}, the number of all exposed persons). In the case of middle-T conditions, such as Case 3, Case 4, and Case 5(20℃, 24℃, 20℃), as the RH increases gradually (30%, 60%, 80%), the R_{max} decreases first and then increase later (3.6 %, 2.1 %, 4.8 %); this may be because the middle RH (45%–60%) is found to be the least favorable for viral survival. Furthermore, in the case of high-RH conditions such as Case 1, Case 5, and Case 6 (90%, 80%, 95%), as the ambient T reduces gradually (40 °C, 20 °C, and 5 °C), the P_V difference in vivo and in

vitro gradually increases (4.27 hPa, 43.4 hPa, 53.8 hPa), and R_{max} also shows a rising trend (2.3%, 4.8%, 5.2%). The large value for Case 6 is evidently due to the low viral inactivation in the air (SARS-CoV-2 was found to survive better at low temperature conditions) and the high deposition fraction in the respiratory tract (the supersaturated air could promote lung deposition due to the ECG effect). This could be another explanation as to why COVID-19 transmission was enhanced in the frozen seafood market, in which the environment is usually cold and damp.

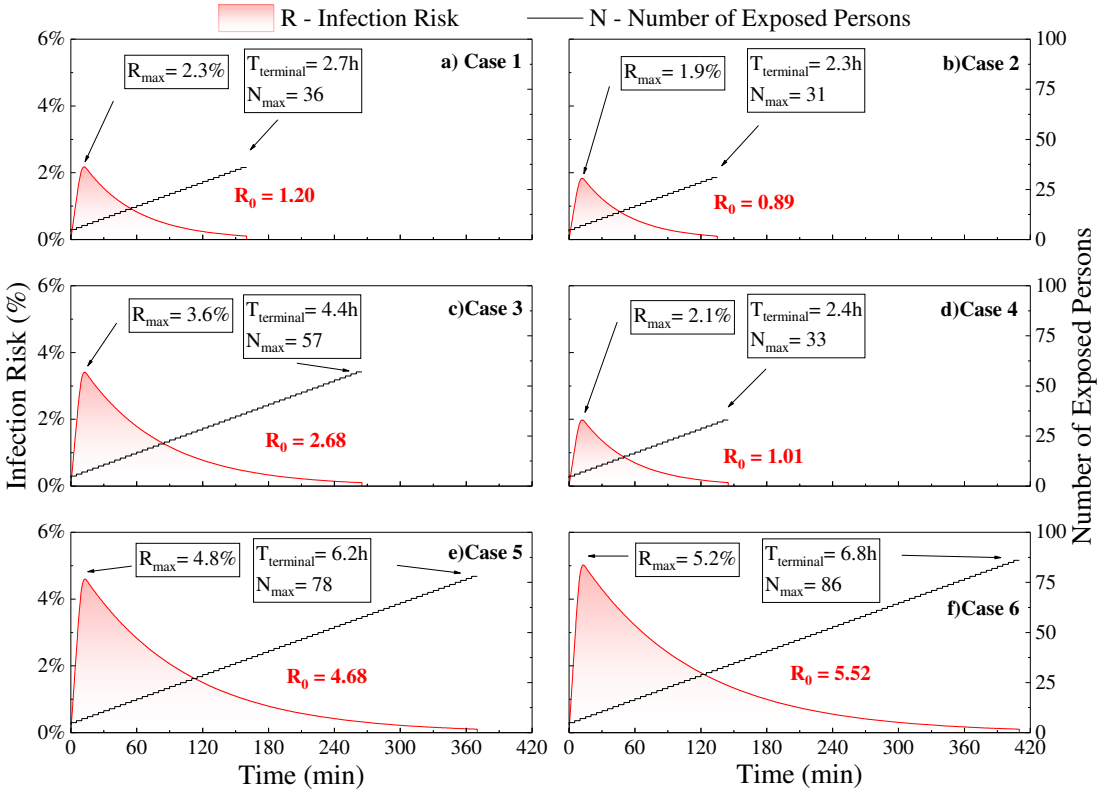

Fig.7 Infection risk (R_{max}) and number of the exposed persons (N_{max}) for all scenarios. The graph shows the brief stopover of the asymptomatic infector (first 5 min) and the high infection risk duration of the microenvironment ($T_{terminal}$). Although the quanta emission rate is consistent in each scenario, viral inactivation in air (λ) and the deposition fraction in the respiratory tract (ω) are significantly influenced by the environment. The highest R_{max} and the longest $T_{terminal}$ might be an explanation as to why COVID-19 transmission was enhanced in the frozen seafood market, in which the environment is usually cold and damp (Case 6).

4. Discussion

It can be concluded from Fig. 8 that people entering the microenvironment around the quanta concentration peak are at a higher risk than those entering after the peak, and each of them received their own risks. Basic reproduction number R_0 is the key index of evaluating the transmission risk of infectious

disease. Fig. 8 shows the comparison between the R_0 simulated by the original W-R model and the R_0' simulated by the modified W-R model.

The original W-R model fails to consider the influence of the environment on viral inactivation and droplet deposition and shows the same result for R_0 in each case, 3.18. However, the R_0' values simulated by the modified W-R model were equal to 1.2, 0.89, 2.68, 1.01, 4.68, and 5.52, respectively. The ratio of the calculated results between the two models (R_0'/R_0) are equal to 38 %, 28 %, 84 %, 32 %, 147 %, and 174 %, respectively. As mentioned earlier, the middle RH (45 %–60 %) and high T (> 30 °C) scenarios were found to be the least favorable to the survival of the viruses, which might be the reason why the disease infection risk is reduced in Cases 1, 2, and 4. The disease infection risk under low-T and high-RH conditions is underestimated by the original model, as in Cases 5 and 6. A higher disease transmission risk is reasonably expected for all indoor environments characterized by low viral inactivation (low T) and high deposition fraction (high RH).

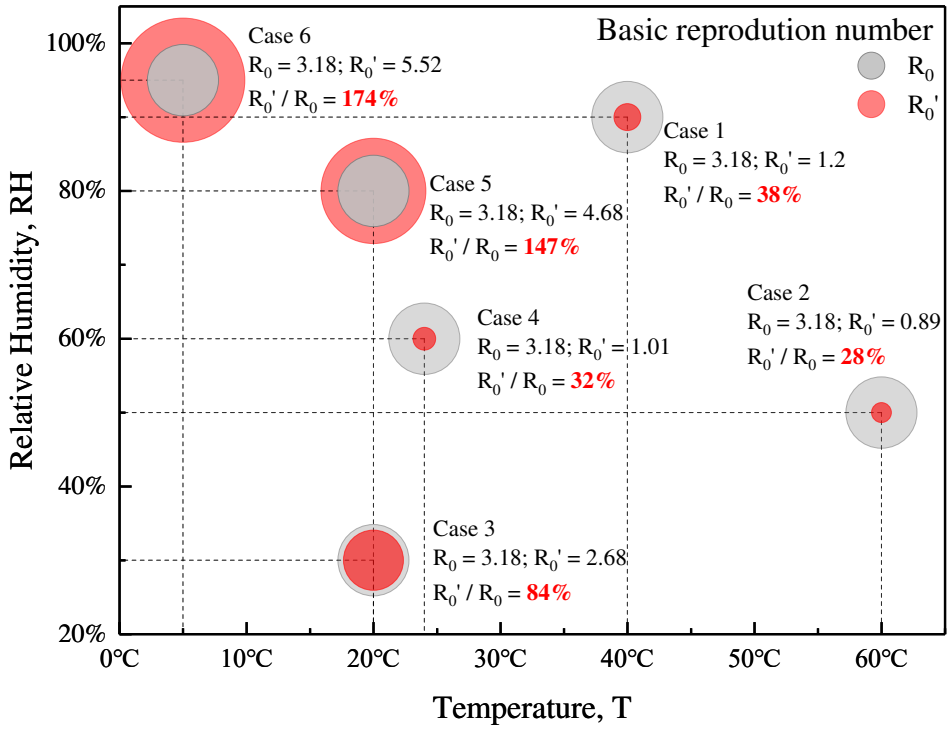

Fig. 8 Comparison between the R_0 simulated by the original W-R model and the R_0' simulated by the modified W-R model. The R_0 for all the exposure scenarios is a constant value, 3.18, since the effects of environmental factors on virus transmission is ignored. Whereas the R_0' changed with the environmental parameters. The disease infection risk under low-T and high-RH conditions is underestimated by the original model, as in Cases 5 and 6.

5. Conclusions

The original W-R model ignored the influence of the environment on viral inactivation and droplet deposition, which might lead to the inappropriate distribution of emergency aid. In addition, to make matters worse, high-risk environments, such as the frozen seafood market, are ill-equipped to effectively control the epidemic due to inadequate information, attention, and action, which may lead to higher risk or something even more catastrophic.

In this study, a new approach is proposed to fill the gaps in knowledge when quantitatively evaluating the influence of environmental parameters on the spread of respiratory tract infections. We analyzed the current available data on the effects of environment on disease infection risk and identified the most critical parameters (T, RH, and P_v), and developed an alternative modified W-R model to address the afore-mentioned problems by proposing the dynamic virus deposition ratio (α) to assess the infection risk under varying environments. Then, it is applied to six typical exposure scenarios in daily life, reflecting how the environmental parameters are linked to viral inactivation and particle deposition, thus quantitatively affecting the transmission risk. In particular, the infection risk in a cold-damp scenario, such as seafood cold store, can reached 6 times higher than in other scenarios at most.

Although we focus here specifically on SARS-CoV-2, this model is equally adaptable to studying the quantitative relationship between environment and the infection risk of any mutated strains of SARS-CoV-2, even other airborne transmission disease. This modified approach will enable healthcare workers and disinfection equipment to be assigned to high-risk environment for COVID-19 prevention, before the infection outbreak, rather than passively waiting.

Declarations

- Ethics approval and consent to participate

Not applicable.

- Consent for publication

Not applicable.

- Availability of data and materials

All data used during the study are available from the corresponding author by request.

- Competing interests

The authors declare there are no potential conflicts of interest with respect to the research, authorship, and/or publication of this article.

- Funding

This work was supported by the National Natural Science Foundation of China (52078314).

- Authors' contributions

Ning Mao: Data curation, Writing-Original draft preparation.

Dingkun Zhang: Reviewing and Editing.

Yupei Li: Reviewing and Editing.

Ying Li: Reviewing and Editing.

Jin Li: Reviewing.

Li Zhao: Reviewing.

Qingqin Wang: Reviewing.

Zhu Cheng: Supervision.

Yin Zhang: Supervision.

Enshen Long: Conceptualization, Methodology, Supervision.

- Authors' information

Ning Mao: cdmaoning@qq.com. MS

Dingkun Zhang: zhangdk14@tsinghua.org.cn. PHD

Yupei Li: sculyp@163.com. MS

Ying Li: 1220884690@qq.com. MS

Jin Li: hvaclijin@163.com. MS

Li Zhao: Zhaolicabr@163.com. PHD

Qingqin Wang: wngqq@cabr.com.cn. PHD

Zhu Cheng: scchengzhu@126.com. PHD

Yin Zhang: cdzhangyin@163.com. PHD

Corresponding author: Enshen Long: longes2@163.com. PHD

References

Adams WC (1993): Measurement of breathing rate and volume in routinely performed daily activities. final report, Human Performance Lab, California University

Akhbarizadeh R, Dobaradaran S, Torkmahalle A (2021): Suspended fine particulate matter (PM2.5), microplastics (MPs), and polycyclic aromatic hydrocarbons (PAHs) in air: Their possible relationships and health implications. ENVIRON REShttps://doi.org/10.1016/j.envres.2020.110339

Alfano FRdA, Dell'Isola M, Ficco G, Tassini F (2012): Experimental analysis of air tightness in Mediterranean buildings using the fan pressurization method. BUILD ENVIRON 53, 16-25, https://doi.org/10.1016/j.buildenv.2011.12.017

Asgari M, Lucci F, Kuczaj AK (2019): Multispecies aerosol evolution and deposition in a bent pipe. J AEROSOL SCI 129, 53-70, https://doi.org/10.1016/j.jaerosci.2018.12.007

Austin E, Brock J, Wissler E (2010): A model for deposition of stable and unstable aerosols in the human respiratory tract. AM IND HYG ASSOC Jhttps://doi.org/10.1080/15298667991430703

Azman AS, Luquero FJ (2020): From China: hope and lessons for COVID-19 control. LANCET INFECT DIS 20, 756-757, https://doi.org/10.1016/S1473-3099(20)30264-4

Bin, Shu-Cheng, Zang, Shi-Ze, Jing-Ru, Guo, Jian-Fa, Wang, Li-Ping, Zhang (2018): HMGB1-Mediated Differential Response on Hippocampal Neurotransmitter Disorder and Neuroinflammation in Adolescent Male and Female Mice following Cold Exposure. BRAIN BEHAV IMMUNhttps://doi.org/10.1016/j.bbi.2018.11.313

Borro L, Mazzei L, Raponi M, Piscitelli P, Miani A, Secinaro A (2020): The role of air conditioning in the diffusion of Sars-CoV-2 in indoor environments: A first computational fluid dynamic model, based on investigations performed at the Vatican State Children's hospital. ENVIRON RES, 110343, https://doi.org/10.1016/j.envres.2020.110343

Buonanno G, Stabile L, Morawska L (2020): Estimation of airborne viral emission: Quanta emission rate of SARS-CoV-2 for infection risk assessment. ENVIRON INT 141, 105794, https://doi.org/10.1016/j.envint.2020.105794

Cao B et al. (2020): A Trial of Lopinavir-Ritonavir in Adults Hospitalized with Severe Covid-19. NEW ENGL J MED 382, 1787-1799, https://doi.org/10.1056/NEJMoa2001282

Chatoutsidou SE, Lazaridis M (2019): Assessment of the impact of particulate dry deposition on soiling of indoor cultural heritage objects found in churches and museums/libraries. J CULT HERIT 39, 221-228, https://doi.org/10.1016/j.culher.2019.02.017

Chen W, Zhang N, Wei J, Yen H, Li Y (2020): Short-range airborne route dominates exposure of respiratory infection during close contact. BUILD ENVIRON 176https://doi.org/10.1016/j.buildenv.2020.106859

China (1998): Public bathhouse Health Standard(GB/ T17220-1998). State Bureau of Technical Supervision of China, pp. 4 (in Chinese)

China (2010): Code for design of cold storage(GB50072-2010). Ministry of housing and urban rural development of China, pp. 135p:A4 (in Chinese)

China (2017): Requirements and evaluation methods of indoor human thermal comfort environment(GB/T 33658-2017). National Standardization Administration Committee, pp. 24 (in Chinese)

Colas de la Noue A, Estienney M, Aho S, Perrier-Cornet JM, de Rougemont A, Pothier P, Gervais P, Belliot G (2014): Absolute Humidity Influences the Seasonal Persistence and Infectivity of Human Norovirus. APPL ENVIRON MICROB 80, 7196-205, https://doi.org/10.1128/AEM.01871-14

Deng L, Ma P, Wu Y, Ma Y, Yang X, Li Y, Deng Q (2020): High and low temperatures aggravate airway inflammation of asthma: Evidence in a mouse model. ENVIRON POLLUT 256, 113433, https://doi.org/10.1016/j.envpol.2019.113433

Doremalen NV, Bushmaker T, Munster V (2013): Stability of Middle East respiratory syndrome coronavirus (MERS-CoV) under different environmental conditions. EUROSURVEILLANCE 18https://doi.org/10.2807/1560-7917.ES2013.18.38.20590

Duguid JP (1946): Expulsion of Pathogenic Organisms from the respiratory tract. BRITISH MEDICAL JOURNAL 1 https://doi.org/10.1136/bmj.1.4442.265

Fierce L, Robey AJ, Hamilton C (2021): Simulating near-field enhancement in transmission of airborne viruses with a quadrature-based model. INDOOR AIR 31, 1843-1859, https://doi.org/10.1111/ina.12900

Franch-Pardo I, Napoletano BM, Rosete-Verges F, Billa L (2020): Spatial analysis and GIS in the study of COVID-19. A review. SCI TOTAL ENVIRON 739, 140033, https://doi.org/10.1016/j.scitotenv.2020.140033

Fröhlich-Nowoisky J, Kampf CJ, Weber B, Huffman JA, Pöhlker C, Andreae MO, Lang-Yona N, Burrows SM, Gunthe SS, Elbert W, Su H, Hoor P, Thines E, Hoffmann T, Després VR, Pöschl U (2016): Bioaerosols in the Earth system: Climate, health, and ecosystem interactions. ATMOS RES 182, 346-376, https://doi.org/10.1016/j.atmosres.2016.07.018

Gammaitoni L, Nucci MC (1997): Using a mathematical model to evaluate the efficacy of TB control measures. EMERG INFECT DIS 3, 335-42, https://doi.org/10.3201/eid0303.970310

Gba B, Ls A, Lm BJEI (2020): Estimation of airborne viral emission: Quanta emission rate of SARS-CoV-2 for infection risk assessment - ScienceDirect. ENVIRON INT 141https://doi.org/10.1016/j.envint.2020.105794

Gralton J, Tovey E, Mclaws ML, Rawlinson WD (2011): The role of particle size in aerosolised pathogen transmission: A review. J INFECTION 62, 1-13, https://doi.org/10.1016/j.jinf.2010.11.010

Guo Y, Qian H, Sun Z, Cao J, Liu F, Luo X, Ling R, Weschler LB, Mo J, Zhang Y (2021): Assessing and controlling infection risk with Wells-Riley model and spatial flow impact factor (SFIF). SUSTAIN CITIES SOC 67, 102719, https://doi.org/10.1016/j.scs.2021.102719

Harper G. J (1961): Airborne micro-organisms: survival tests with four viruses. JOURNAL OF

510 HYGIENE 59, 479, https://doi.org/10.1017/s0022172400039176

511 Harrichandra A, Ierardi AM, Pavilonis B (2020): An estimation of airborne SARS-CoV-2 infection
512 transmission risk in New York City nail salons. TOXICOL IND HEALTH 36, 074823372096465,
513 https://doi.org/10.1177/0748233720964650

514 Ishmatov A (2020): Influence of weather and seasonal variations in temperature and humidity on
515 supersaturation and enhanced deposition of submicron aerosols in the human respiratory tract. ATMOS
516 ENVIRON 223https://doi.org/10.1016/j.atmosenv.2019.117226

517 Keene CH (1955): Airborne Contagion and Air Hygiene. William Firth Wells. 25, 249-249,
518 https://doi.org/10.1111/j.1746-1561.1955.tb08015.x

519 Killerby ME, Biggs HM, Haynes A, Dahl RM, Mustaquim D, Gerber SI, Watson JT (2018):
520 Human coronavirus circulation in the United States 2014-2017. J CLIN VIROL 101, 52-56,
521 https://doi.org/10.1016/j.jcv.2018.01.019

522 Kim JW, Xi J, Si XA (2013): Dynamic growth and deposition of hygroscopic aerosols in the nasal
523 airway of a 5-year-old child. INT J NUMER METH BIO 29, 17-39, https://doi.org/10.1002/cnm.2490

524 Knight V (2010): Viruses as agents of airborne contagion. ANN NY ACAD SCI 353, 147-156,
525 https://doi.org/10.1111/j.1749-6632.1980.tb18917.x

526 Kreyling GAFHG (1984): Conditions for measuring supersaturation in the human lung using
527 aerosols. J AEROSOL SCIhttps://doi.org/10.1016/0021-8502(84)90065-X

528 L. Zou FR, M. Huang, L. Liang, H. Huang, Z. Hong, J. Yu, M. Kang, Y. Song, J. Xia, Q. Guo, T.
529 Song, J. He, H.L. Yen, M. Peiris, J. Wu, (2020): SARS-CoV-2 Viral Load in Upper Respiratory
530 Specimens of Infected Patients. NEW ENGL J MED 382, 1177-1179.,
531 https://doi.org/10.1056/NEJMc2001737

532 Lai CC, Shih TP, Ko WC, Tang HJ, Hsueh PR (2020): Severe acute respiratory syndrome
533 coronavirus 2 (SARS-CoV-2) and coronavirus disease-2019 (COVID-19): The epidemic and the
534 challenges. Int J Antimicrob Agents 55, 105924, https://doi.org/10.1016/j.ijantimicag.2020.105924

535 Li Y, Duan S, Yu ITS, Wong TWJ (2010): Multi-zone modeling of probable SARS virus
536 transmission by airflow between flats in Block E, Amoy Gardens. INDOOR AIR 15, 96-111,
537 https://doi.org/10.1111/j.1600-0668.2004.00318.x

538 Lin C, Lau AKH, Fung JCH, Guo C, Chan JWM, Yeung DW, Zhang Y, Bo Y, Hossain MS, Zeng
539 Y, Lao XQ (2020): A mechanism-based parameterisation scheme to investigate the association between
540 transmission rate of COVID-19 and meteorological factors on plains in China. SCI TOTAL ENVIRON
541 737, 140348, https://doi.org/10.1016/j.scitotenv.2020.140348

542 Lin K, Marr LC (2020): Humidity-Dependent Decay of Viruses, but Not Bacteria, in Aerosols and
543 Droplets Follows Disinfection Kinetics. ENVIRON SCI TECHNOL 54, 1024-1032,
544 https://doi.org/10.1021/acs.est.9b04959

545 Lindsley WG, Pearce TA, Hudnall JB, Davis KA, Davis SM, Fisher MA, Khakoo R, Palmer JE,
546 Clark KE, Celik I, Coffey CC, Blachere FM, Beezhold DH (2012): Quantity and size distribution of

547 cough-generated aerosol particles produced by influenza patients during and after illness. J OCCUP
548 ENVIRON HYG 9, 443-9, https://doi.org/10.1080/15459624.2012.684582

549 Lipsitch M, Swerdlow DL, Finelli L (2020): Defining the Epidemiology of Covid-19 — Studies
550 Needed. NEW ENGL J MED 382https://doi.org/10.1056/NEJMp2002125

551 Liu J, Zhou J, Yao J, Zhang X, Li L, Xu X, He X, Wang B, Fu S, Niu T, Yan J, Shi Y, Ren X, Niu
552 J, Zhu W, Li S, Luo B, Zhang K (2020a): Impact of meteorological factors on the COVID-19
553 transmission: A multi-city study in China. SCI TOTAL ENVIRON 726, 138513,
554 https://doi.org/10.1016/j.scitotenv.2020.138513

555 Liu Y, Ning Z, Chen Y, Guo M, Liu Y, Gali NK, Sun L, Duan Y, Cai J, Westerdahl D, Liu X, Ho
556 K-f, Kan H, Fu Q, Lan K (2020b): Aerodynamic Characteristics and RNA Concentration of SARS-
557 CoV-2 Aerosol in Wuhan Hospitals during COVID-19 Outbreak.
558 BioRxivhttps://doi.org/10.1101/2020.03.08.982637

559 Longest PW, Hindle M (2010): CFD simulations of enhanced condensational growth (ECG)
560 applied to respiratory drug delivery with comparisons to in vitro data. J AEROSOL SCI 41, 805-820,
561 https://doi.org/10.1016/j.jaerosci.2010.04.006

562 Longest PW, Hindle M (2011): Numerical Model to Characterize the Size Increase of
563 Combination Drug and Hygroscopic Excipient Nanoparticle Aerosols. AEROSOL SCI TECH 45, 884-
564 899, https://doi.org/10.1080/02786826.2011.566592

565 Longest PW, Tian G, Hindle M (2011): Improving the lung delivery of nasally administered
566 aerosols during noninvasive ventilation-an application of enhanced condensational growth (ECG). J
567 AEROSOL MED PULM D 24, 103-18, https://doi.org/10.1089/jamp.2010.0849

568 Ma Y, Zhao Y, Liu J, He X, Wang B, Fu S, Yan J, Niu J, Zhou J, Luo B (2020): Effects of
569 temperature variation and humidity on the death of COVID-19 in Wuhan, China. SCI TOTAL
570 ENVIRON 724, 138226, https://doi.org/10.1016/j.scitotenv.2020.138226

571 Mao N, An CK, Guo LY, Wang M, Guo L, Guo SR, Long ES (2020): Transmission risk of
572 infectious droplets in physical spreading process at different times: A review. BUILD ENVIRON
573 185https://doi.org/10.1016/j.buildenv.2020.107307

574 Marmett B, Pires Dorneles G, Boek Carvalho R, Peres A, Roosevelt Torres Romao P, Barcos
575 Nunes R, Ramos Rhoden C (2020): Air pollution concentration and period of the day modulates
576 inhalation of PM2.5 during moderate- and high-intensity interval exercise. ENVIRON RES, 110528,
577 https://doi.org/10.1016/j.envres.2020.110528

578 McClymont H, Hu W (2021): Weather Variability and COVID-19 Transmission: A Review of
579 Recent Research. INT J ENV RES PUB HE 18https://doi.org/10.3390/ijerph18020396

580 Morawska L, Johnson GR, Ristovski ZD, Hargreaves M, Mengersen K, Corbett S, Chao CYH, Li
581 Y, Katoshevski D (2009): Size distribution and sites of origin of droplets expelled from the human
582 respiratory tract during expiratory activities. J AEROSOL SCI 40, 256-269,
583 https://doi.org/10.1016/j.jaerosci.2008.11.002

584 Morawska L et al. (2020): How can airborne transmission of COVID-19 indoors be minimised?

585 Environment International 142https://doi.org/10.1016/j.envint.2020.105832

586 Morrow PE (2010): Physics of airborne particles and their deposition in the lung. ANN NY ACAD
587 SCI 353, 71-80, https://doi.org/10.1111/j.1749-6632.1980.tb18908.x

588 Nan ZH, Li Z, Yang SS, Jun T, Hong CZ (2009): Seasonal Characteristics of Clinical Rate of
589 Influenza-Like Illness in Shenzhen and Its Meteorological Forecast Model. Meteorological science and
590 technology 37, 709-712, https://doi.org/10.3969/j.issn.1671-6345.2009.06.014 (in Chinese)

591 Nicas M, Hubbard WWN, Alan (2005): Toward Understanding the Risk of Secondary Airborne
592 Infection: Emission of Respirable Pathogens. J OCCUP ENVIRON
593 HYGhttps://doi.org/10.1080/15459620590918466

594 Nordsiek F, Bodenschatz E, Bagheri G (2021): Risk assessment for airborne disease transmission
595 by poly-pathogen aerosols. PLoS One 16, e0248004, https://doi.org/10.1371/journal.pone.0248004

596 Noti JD, Blachere FM, McMillen CM, Lindsley WG, Kashon ML, Slaughter DR, Beezhold DH
597 (2013): High humidity leads to loss of infectious influenza virus from simulated coughs. PLoS One 8,
598 e57485, https://doi.org/10.1371/journal.pone.0057485

599 Pani SK, Lin N-H, RavindraBabu S (2020): Association of COVID-19 pandemic with
600 meteorological parameters over Singapore. SCI TOTAL ENVIRON
601 740https://doi.org/10.1016/j.scitotenv.2020.140112

602 Pica N, Bouvier NMJCOiV (2012): Environmental factors affecting the transmission of
603 respiratory viruses. 2, 90-95, https://doi.org/10.1016/j.coviro.2011.12.003

604 Prata DN, Rodrigues W, Bermejo PH (2020): Temperature significantly changes COVID-19
605 transmission in (sub)tropical cities of Brazil. SCI TOTAL ENVIRON 729, 138862,
606 https://doi.org/10.1016/j.scitotenv.2020.138862

607 Protection ICoR (1994): Summary description of respiratory tract dosimetry model. Annals of the
608 ICRP 24, 106–120, https://doi.org/10.1016/0146-6453(94)90038-8

609 Pu X, Wang L, Chen L, Pan J, Tang L, Wen J, Qiu H (2020): Differential effects of size-specific
610 particulate matter on lower respiratory infections in children: A multi-city time-series analysis in
611 Sichuan, China. ENVIRON RES 193, 110581, https://doi.org/10.1016/j.envres.2020.110581

612 Pyankov OV, Bodnev SA, Pyankova OG, Agranovski IE (2018): Survival of aerosolized
613 coronavirus in the ambient air. J AEROSOL SCI 115, 158-163,
614 https://doi.org/10.1016/j.jaerosci.2017.09.009

615 Qian H, Zheng XH, Zhang XJ (2012): Prediction model of air borne infection probability of
616 respiratory infectious diseases JOURNAL OF SOUTHEAST UNIVERSITY (Natural Science
617 Edition） 42, 468-472 https://doi.org/10.3969/j.issn.1001—0505.2012.03.014 (in Chinese)

618 Riley EC, Murphy G, Riley RL (1978): Airborne spread of measles in a suburban elementary
619 school. AM J EPIDEMIOL, 421-32, https://doi.org/10.1371/journal.pone.0002691

620 Rothman KJ, Greenland S, Lash TL (2011): Modern epidemiology: Third edition, 1-758 pp

621 Runkle JD, Sugg MM, Leeper RD, Rao Y, Matthews JL, Rennie JJ (2020): Short-term effects of
622 specific humidity and temperature on COVID-19 morbidity in select US cities. SCI TOTAL ENVIRON
623 740, 140093, https://doi.org/10.1016/j.scitotenv.2020.140093

624 Sarangapani R, Wexler AS (1996): Growth and neutralization of sulfate aerosols in human
625 airways. J AEROSOL SCI 81, 480-490, https://doi.org/10.1055/s-2007-972910

626 Sattar S, Ijaz MK, Johnson-Lussenburg C, Springthorpe V (1984): Effect of relative humidity on
627 the airborne survival of rotavirus SAII. https://doi.org/10.1128/AEM.47.4.879-881.1984

628 Sharma R, Balasubramanian R (2020): Evaluation of the effectiveness of a portable air cleaner in
629 mitigating indoor human exposure to cooking-derived airborne particles. ENVIRON RES
630 183https://doi.org/10.1016/j.envres.2020.109192

631 Sobral MFF, Duarte GB, da Penha Sobral AIG, Marinho MLM, de Souza Melo A (2020):
632 Association between climate variables and global transmission oF SARS-CoV-2. SCI TOTAL
633 ENVIRON 729, 138997, https://doi.org/10.1016/j.scitotenv.2020.138997

634 Stabile L, Dell'Isola M, Russi A, Massimo A, Buonanno G (2017): The effect of natural
635 ventilation strategy on indoor air quality in schools. SCI TOTAL ENVIRON 595, 894-902,
636 https://doi.org/10.1016/j.scitotenv.2017.03.048

637 Tian G, Longest PW, Su G, Hindle M (2011): Characterization of Respiratory Drug Delivery with
638 Enhanced Condensational Growth using an Individual Path Model of the Entire Tracheobronchial
639 Airways. ANN BIOMED ENG 39, 1136-1153, https://doi.org/10.1007/s10439-010-0223-z

640 Urrego J, Ko AI, da Silva Santos Carbone A, Paiao DS, Sgarbi RV, Yeckel CW, Andrews JR,
641 Croda J (2015): The Impact of Ventilation and Early Diagnosis on Tuberculosis Transmission in
642 Brazilian Prisons. AM J TROP MED HYG 93, 739-46, https://doi.org/10.4269/ajtmh.15-0166

643 van Doremalen N, Bushmaker T, Morris DH, Holbrook MG, Gamble A, Williamson BN, Tamin
644 A, Harcourt JL, Thornburg NJ, Gerber SI, Lloyd-Smith JO, de Wit E, Munster VJ (2020): Aerosol and
645 Surface Stability of SARS-CoV-2 as Compared with SARS-CoV-1. NEW ENGL J MED 382, 1564-
646 1567, https://doi.org/10.1056/NEJMc2004973

647 Vuorinen V et al. (2020): Modelling aerosol transport and virus exposure with numerical
648 simulations in relation to SARS-CoV-2 transmission by inhalation indoors. SAF SCI 130, 104866,
649 https://doi.org/10.1016/j.ssci.2020.104866

650 Wagner BG, Coburn BJ, Blower S (2009): Calculating the potential for within-flight transmission
651 of influenza A (H1N1). BMC MED 7, 81, https://doi.org/10.1186/1741-7015-7-81

652 Walsh KA, Jordan K, Clyne B, Rohde D, Drummond L, Byrne P, Ahern S, Carty PG, O'Brien KK,
653 O'Murchu E, O'Neill M, Smith SM, Ryan M, Harrington P (2020): SARS-CoV-2 detection, viral load
654 and infectivity over the course of an infection. J INFECTION 81, 357-371,
655 https://doi.org/10.1016/j.jinf.2020.06.067

656 Wang J, Tang K, Feng K, Lin X, Lv W, Chen K, Wang F (2020): High Temperature and High
657 Humidity Reduce the Transmission of COVID-19. Social science Electronic
658 Publishinghttps://doi.org/10.2139/ssrn.3551767

659 Watanabe T, Bartrand TA, Weir MH, Omura T, Haas CN (2010): Development of a Dose-
660 Response Model for SARS Coronavirus. RISK ANAL 30, 1129-1138, https://doi.org/10.1111/j.1539-
661 6924.2010.01427.x

662 Wei J, Li YJAAJoIC (2016): Airborne spread of infectious agents in the indoor environment. 44,
663 S102-S108, https://doi.org/10.1016/j.ajic.2016.06.003

664 Winkler-Heil R, Pichelstorfer L, Hofmann W (2017): Aerosol dynamics model for the simulation
665 of hygroscopic growth and deposition of inhaled NaCl particles in the human respiratory tract. J
666 AEROSOL SCI 113, 212-226, https://doi.org/10.1016/j.jaerosci.2017.08.005

667 Wu Y, Jing W, Liu J, Ma Q, Yuan J, Wang Y, Du M, Liu M (2020): Effects of temperature and
668 humidity on the daily new cases and new deaths of COVID-19 in 166 countries. SCI TOTAL
669 ENVIRON 729, 139051, https://doi.org/10.1016/j.scitotenv.2020.139051

670 Xi J, Kim J, Si XA, Zhou Y (2013): Hygroscopic aerosol deposition in the human upper
671 respiratory tract under various thermo-humidity conditions. J Environ Sci Health A Tox Hazard Subst
672 Environ Eng 48, 1790-805, https://doi.org/10.1080/10934529.2013.823333

673 Xi J, Si XA, Kim JW (2015): Chapter 5. Characterizing Respiratory Airflow and Aerosol
674 Condensational Growth in Children and Adults Using an Imaging-CFD Approach. Elsevier Inc, 125-
675 155, https://doi.org/10.1016/b978-0-12-408077-5.00005-5

676 Xu H, Yan C, Fu Q, Xiao K, Yu Y, Han D, Wang W, Cheng J (2020): Possible environmental
677 effects on the spread of COVID-19 in China. SCI TOTAL ENVIRON 731, 139211,
678 https://doi.org/10.1016/j.scitotenv.2020.139211

679 Y. Pan DZ, P. Yang, L.L.M. Poon, Q. Wang, (2020): Viral load of SARS-CoV-2 in clinical
680 samples. LANCET INFECT DIS 4, 411-412., https://doi.org/10.1016/S1473-3099(20)30113-4

681 Yan C (2015): Experimental study on indoor thermal environment of residential buildings in
682 North China in winter. Shanxi Architecture 41, 198-199 (in Chinese),
683 https://doi.org/CNKI:SUN:JZSX.0.2015-35-109

684 Yeh HC, Raabe RFPG (1976): Factors influencing the deposition of inhaled particles. ENVIRON
685 HEALTH PERSP 15, 147-156, https://doi.org/10.2307/3428398

686 Yu ITS, Li Y, Wong TW, Tam W, Chan AT, Lee J, W. H (2004): Evidence of Airborne
687 Transmission of the Severe Acute Respiratory Syndrome Virus. NEW ENGL J MED 17, 1731–1739,
688 https://doi.org/10.1056/NEJMoa032867

689 Zhai Z, Li H (2021): Distributed probability of infection risk of airborne respiratory diseases.
690 INDOOR BUILT ENVIRONhttps://doi.org/10.1177/1420326x211030324

691 Zhang X, Ji Z, Yue Y, Liu H, Wang J (2020): Infection Risk Assessment of COVID-19 through
692 Aerosol Transmission: a Case Study of South China Seafood Market. ENVIRON SCI
693 TECHNOLhttps://doi.org/10.1021/acs.est.0c02895

694 Zhou J, Koutsopoulos HN (2021): Virus Transmission Risk in Urban Rail Systems: Microscopic
695 Simulation-Based Analysis of Spatio-Temporal Characteristics. Transportation Research Record:

Journal of the Transportation Research Board 2675, 120-132 (in Chinese), https://doi.org/10.1177/03611981211010181

Supplementary Files

This is a list of supplementary files associated with this preprint. Click to download.

- AppendixA.Fig.1Diametergrowthfactor.tif
- 4.5SupplementarymaterialAppendixAofthispaper.docx